POAC'15
Trondheim, Norway

Proceedings of the 23rd International Conference on
Port and Ocean Engineering under Arctic Conditions
June 14-18, 2015
Trondheim, Norway

An efficient method for computing the time domain response of a floating ice block including hydrodynamics

Chris Keijdener [1,2], Andrei Metrikine [1,2]
[1]Delft University of Technology, Delft, the Netherlands
[2] SAMCoT, NTNU, Trondheim, Norway

ABSTRACT

When studying the dynamics of ice-structure interaction, hydrodynamic effects are often ignored to simplify the model. One of the challenges associated with the introduction of the hydrodynamic forces is that those introduce frequency dependent added mass and damping into the system. In order to include these two components in a time domain model with a non-linear contact model, a convolution integral is needed to compute the response of the body. Computing the convolution integral is computationally intensive and as such undesired.

In this paper a methodology is presented which allows the time domain response of a floating ice block (a rigid body) to be computed, including the effects of hydrodynamics, without having to resort to using a convolution integral. This is done by approximating the complex frequency response of the floating body with that of an equivalent dynamical system. By choosing a replacement system whose time domain representation can be readily solved with an ODE solver, the time domain response of the original floating ice block can be obtained without having to evaluate a convolution integral. Ultimately, a replacement system with only three degrees of freedom is needed to compute the time domain response of the floating block of ice with an error in the heave motion of about 0.1%.

INTRODUCTION

Studies on the interaction between a floating ice sheets and floating offshore structures have been ongoing for many years. In most studies this interaction process is considered to be quasi-static. However, when dealing with the interaction between ice and floating structures, the relative velocities can become high enough to violate the quasi-static assumption. During these high speed interactions, time dependent effects can no longer be ignored and need to be properly accounted for in order to accurate model the interaction process (Keijdener & Metrikine, 2014). There are two main sources of time dependent effects, namely due to the mass of the ice itself and due to hydrodynamics. The ice related ones are generally included in models concerned with dynamics whilst the hydrodynamic ones are not. In this paper a first step is made towards including hydrodynamics so that its effects on the interaction can be studied.

The topic of hydrodynamics is certainly not unknown within the field of arctic engineering. It has been studied extensively in light of the attenuation of ocean waves as they travel through ice infested waters (Squire, 2007). There have also been various studies on the hydrodynamic coupling of vessel of ice rubble motions (Isaacson & McTaggart, 1990; Tsarau, Lubbad, & Løset, 2014). However, in these models there is no direct contact between the ice and the structure.

Taking a step back to ice-floater interaction in general, two types of models can be identified, namely analytical and numerical. When dealing with dynamics the required contact model often becomes non-linear and so analytical models are no longer an option. However, currently there are only very few numerical models aimed at modelling the ice-floater interaction which also include the effects of hydrodynamics. There have been some studies related to iceberg impacts (Gagnon & Wang, 2012; Kim, Storheim, von Bock und Polach, & Amdahl, 2012) and another study on the effects of ventilation and back-fill (Lu, Løset, & Lubbad, 2012). However, all these studies were based on computationally intensive models.

In this paper a first step is taken towards developing a numerically efficient way to include hydrodynamics in ice-floater interaction models. The principle idea is explained in this paper by deriving a fast time-domain model for a single piece of ice rubble. Even though the ice rubble is assumed to be rigid, it serves as a good starting point for the more complicated case when the ice is allowed to be elastic as in that case the resulting forcing on the ice is not only frequency dependent, but also wavenumber dependent. However, the rigid case covered in this paper is still valid for relatively small ice floes as those behave rigid and as such is also relevant on its own.

The hydrodynamics has a strong influence on the heave and pitch motion of the block. Due to the limited number of pages allowed, this paper only covers the heave motion of the block. However, the procedure is exactly the same when applied to the pitch motion except that the force now has an arm. In addition, the derivation is only done for single block. If other blocks or a floating vessel is present the hydrodynamics of all these floating objects will be coupled. This will complicated the procedure described in this paper. As this paper is a first step, only a single block is considered.

In the first part of this paper the frequency domain response (FDR) of the ice block is derived. In the second part a fast way to compute its time domain response is presented.

DERIVATION OF THE ICE BLOCK'S FREQUENCY DOMAIN RESPONSE

Before the FDR of the floating ice block can be approximated with that of the replacement system, the FDR of the rigid body (ice block) has to be derived. This is done next using a semi-analytical approach. The problem to be solved is illustrated in Figure 1.

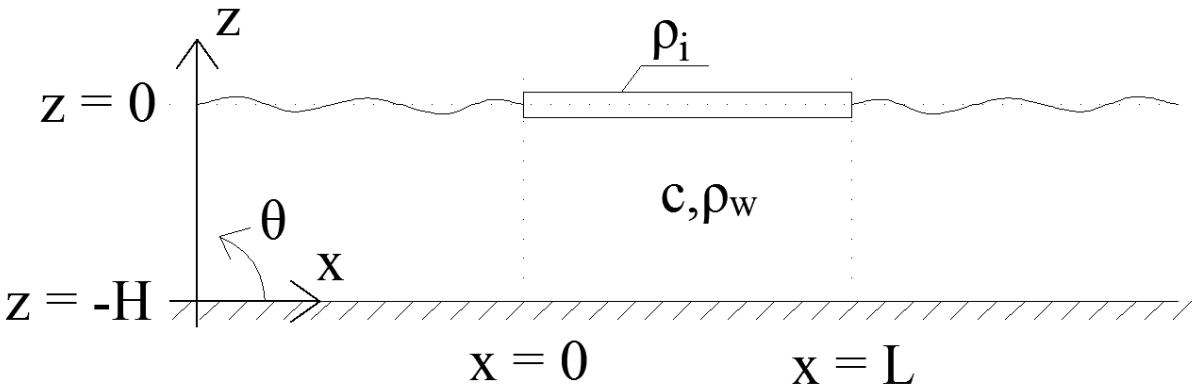

Figure 1: Problem definition

The equation of motion (EoM) of the fluid is

$$\ddot{\phi} - c^2 \Delta\phi = 0, \qquad \forall \;\; x \in (-\infty, \infty) \;\; \cap \;\; z \in (-H, 0) \tag{1}$$

where the velocity potential ϕ is a function of x,z and t, the dot accent denotes derivatives with respect to time, c is the compressive wave speed of the fluid and Δ is the Laplace operator. The boundary condition at the seafloor is

$$\phi_{,z}\big|_{z=-H} = 0 \tag{2}$$

where $_{,z}$ denotes a derivative with respect to z and H is the water depth. The boundary condition at the surface, including the interface with the rigid body, is

$$\ddot{\phi}\big|_{z=0} + g\phi_{,z}\big|_{z=0} = 0, \qquad \forall\, x \notin [0, L] \tag{3}$$

$$\phi_{,z}\big|_{z=0} = \dot{W}, \qquad \forall\, x \in [0, L] \tag{4}$$

where g is the gravitational constant and W is the displacement of the body whose EoM is given by

$$m\ddot{W}(t) = \int_0^L p(\bar{x}, 0, t)\, d\bar{x} + \delta(t) \tag{5}$$

where the $\bar{}$ denotes variables which are internal to the integral and $\delta(t)$ is the Dirac delta function. The delta function is used for the external force as this will result in the fundamental solution of the system. The pressure p in the fluid has the following linearized form

$$p(x, z, t) = -\rho_w b\left(\dot{\phi} + gz\right) \tag{6}$$

where ρ_w is the density of the fluid and b is the width of the body. Since the pressure is evaluated at $z = 0$ in the EoM of the body (Eq. 5), the hydrostatic pressure ($-\rho_w bgz$) at this depth is equal to the displacement of the body. Combining the last three equations, the body's EoM can be rewritten as

$$m\ddot{W}(t) = \int_0^L -\rho_w b \left(\dot{\phi}_{,z}(\bar{x}, z, t)\big|_{z=0} + g \int_0^t \phi_{,z}(\bar{x}, z, \tau)\big|_{z=0}\, d\tau \right) d\bar{x} + \delta(t) \tag{7}$$

Finding the general solution of the fluid

The first step in getting the FDR is to solve the fluid domain. This is done by assuming the following solution for the potential ϕ

$$\phi(x, z, t) = \tilde{\phi}(x, z, \omega) e^{i\omega t} \tag{8}$$

where ω is the frequency and the tilde accent denotes a transformed variable. This is substituted in the EoM of the fluid (Eq. 1) to get

$$-\omega^2 \tilde{\phi} - c^2 \Delta \tilde{\phi} = 0, \qquad \forall \;\; x \in (-\infty, \infty) \;\; \cap \;\; z \in (-H, 0) \tag{9}$$

Next, the integral Fourier transform (Eq. 11) is applied along the x-direction to obtain the following ordinary differential equation (ODE) for $\tilde{\tilde{\phi}}$

$$-\omega^2 \tilde{\tilde{\phi}} - c^2 \left(\tilde{\tilde{\phi}}_{,zz} - k^2 \tilde{\tilde{\phi}} \right) = 0, \qquad \forall \;\; z \in (-H, 0) \tag{10}$$

$$\tilde{f}(\omega) = \int_{-\infty}^{\infty} f(t) e^{-i\omega t} dt\,, \qquad f(t) = \frac{1}{2\pi} \int_{-\infty}^{\infty} \tilde{f}(\omega) e^{i\omega t} d\omega \tag{11}$$

Solving this ODE and applying the boundary condition at the seafloor results in the following expression

$$\tilde{\tilde{\phi}}(k,z,\omega)=\frac{\cos\big(\lambda(z+H)\big)}{\cos(\lambda H)}A(k,\omega),\qquad \forall\ z\in[-H,0),\qquad \lambda=\sqrt{\frac{\omega^2}{c^2}-k^2} \tag{12}$$

where k is the wavenumber in horizontal direction, λ is the wavenumber is vertical direction and $A(k,\omega)$ is the complex amplitude. Using this result, the expression for the interaction pressure, given by Eq 6, can be rewritten to become

$$\tilde{\tilde{p}}(k,0,\omega)=-\frac{\rho_w b}{i\omega}(-\omega^2-g\lambda\tan(\lambda H))A(k,\omega)=-\rho_w bQ(\omega,k)A(k,\omega) \tag{13}$$

where $A(k,\omega)$ is the only unknown.

Discretization of the pressure at the interface

Now that fluid domain satisfies its boundaries and its pressures can be computed, the focus can shift to the fluid pressures at the interface with the body. This will make it possible to find the unknown amplitude of the potential, $A(k,\omega)$.

In order to find the amplitude, the assumption is made that the interface pressure can be expressed as a summation of unknown forcing functions, $F_n(\omega)$, analogous to D'Alembert's principle. The mathematical expression as well as an illustration are given below.

$$\tilde{p}^*(x,0,\omega) = \sum_{n=1}^{N} \frac{F_n(\omega)}{\Delta x} H\left(\frac{\Delta x}{2} - |x - x_n|\right), \qquad x_n = \Delta x \frac{(2n-1)}{2}, \qquad \Delta x = \frac{L}{N} \tag{14}$$

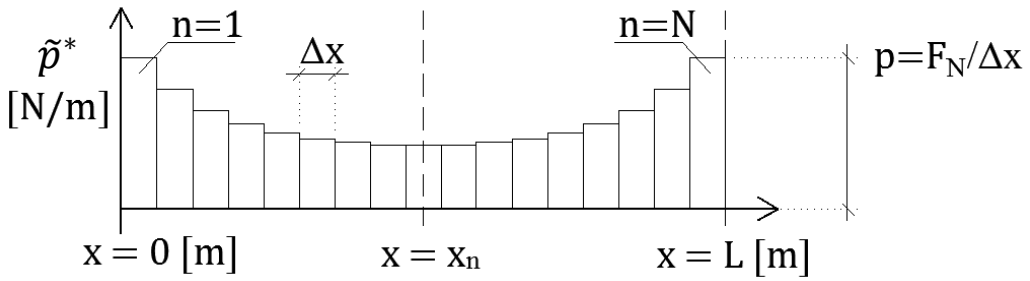

Figure 2: An illustration of the discretized interaction pressure $\tilde{p}^*$ as given by Eq. 14. Note that the pressure is zero if $x \notin [0, L]$.

where $H(..)$ is the Heaviside function, n is the element-id, Δx is equivalent to an element size, x_n is the centre of each element and N is the total number of elements. The free-surface boundary condition given by Eq. 3 is included correctly in the assumed formulation because the surface pressure outside the domain of the rigid body is equal to zero. Application of the integral Fourier transform over x on this expression gives

$$\tilde{\tilde{p}}^*(k,0,\omega) = \sum_{n=1}^{N} F_n(\omega)\, \Upsilon_n(k), \qquad \Upsilon_n(k) = \frac{1}{\Delta x} \int_{-\infty}^{\infty} H\left(\frac{\Delta x}{2} - |\bar{x} - x_n|\right) e^{-ik\bar{x}}\, d\bar{x} \tag{15}$$

By equating the "exact" ($\tilde{\tilde{p}}$) and assumed form ($\tilde{\tilde{p}}^*$) of the interface pressure, a relation between the unknown amplitude $A(k,\omega)$ and the unknown forcing functions is obtained

$$A(k,\omega) = \frac{\sum_{n=1}^{N} F_n(\omega)\, \Upsilon_n(k)}{-\rho_w b Q(\omega,k)} \tag{16}$$

With this step the unknown has shifted from the amplitude of the potential $A(k,\omega)$ to the amplitude of the interface forces $F_n(\omega)$.

Equation of motion of the rigid body

With the interaction pressure discretized, the focus can finally shift to the rigid body. With its EoM an expression for the unknown amplitude of the interface forces $F_n(\omega)$ can be obtained. To start, the assumed form of the interaction pressure is substituted into the EoM of the body (Eq. 5). After this, the EoM is transformed to the frequency domain to get

$$-m\omega^2\widetilde{W} = \int_0^L \tilde{p}^*(\bar{x}, 0, \omega)\, d\bar{x} + 1 \tag{17}$$

The integral on the right-hand side is now evaluated. The domain of each F_n has a width of Δx as can be seen in Figure 2. Since each F_n is constant within its domain, the integral over each Heaviside function results in a multiplication with Δx. This gives $\Delta x/\Delta x$ and so the EoM becomes

$$-m\omega^2\widetilde{W} = \sum_{n=1}^{N} F_n(\omega) + 1 \tag{18}$$

At this point the kinematic continuity condition given by Eq. 4 is needed to express the displacements of the rigid body, $\widetilde{W}$, in terms of the potential.

The condition in its original form is continuous and applies to any value of x which falls within the domain of the body. The condition is very strong and need not be enforced on the current system. Because of this, the condition is relaxed by saying that it only has to hold at certain points. As there are N unknown F_n's, N equation are needed to find them. As such the kinematic condition is enforced at N points to obtain N equations. As the fluid is continues, a representative value has to be used for each point. The value used for each point is the average fluid velocity of the element associated with that particular point. Mathematically the relaxed condition can be expressed as

$$i\omega\widetilde{W} = \tilde{\phi}_{,z}\big|_{z=0}, \qquad \forall\, x \in [0, L] \quad \rightarrow \quad i\omega\widetilde{W} = \frac{1}{\Delta x}\int_{(\alpha-1)\Delta x}^{\alpha\Delta x} \tilde{\phi}_{,z}(\bar{x}, 0, \omega)\, d\bar{x}, \qquad \forall\ \alpha = 1..N \tag{19}$$

where α is the identifier for each equation. This result is now substituted back into the EoM of the body (Eq. 18) to get

$$\frac{i\omega m}{\Delta x}\int_{(\alpha-1)\Delta x}^{\alpha\Delta x} \tilde{\phi}_{,z}(x, 0, \omega)\, dx = \sum_{n=1}^{N} F_n(\omega) + 1 \tag{20}$$

$\tilde{\phi}_{,z}$ on the left hand side can be rewritten using the definition of the inverse Fourier transform (Eq. 11) in combination with the previously found expression for $\tilde{\tilde{\phi}}$ (Eq. 12) to get

$$-\frac{i\omega m}{2\pi}\frac{1}{\Delta x}\int_{(\alpha-1)\Delta x}^{\alpha\Delta x}\int_{-\infty}^{\infty} A(k, \omega)\lambda \tan(\lambda H)\, e^{ikx}\, dk\, dx = \sum_{n=1}^{N} F_n(\omega) + 1, \qquad \forall\ \alpha = 1..N \tag{21}$$

The integral over x is solved

$$-\frac{i\omega m}{2\pi}\frac{1}{\Delta x}\int_{-\infty}^{\infty} A(k, \omega)\lambda \tan(\lambda H)\frac{1}{ik}\left(e^{ik\alpha\Delta x} - e^{ik(\alpha-1)\Delta x}\right) dk = \sum_{n=1}^{N} F_n(\omega) + 1, \qquad \forall\ \alpha = 1..P \tag{22}$$

Next the integral over the Heaviside function $\Upsilon_n(k)$ is solved

$$\Upsilon_n(k) = \frac{1}{\Delta x}\int_{-\infty}^{\infty} H\left(\frac{\Delta x}{2} - |\bar{x} - x_n|\right) e^{-ik\bar{x}}\, d\bar{x} = \frac{i}{\Delta x}\frac{1}{k}\left(e^{-ikn\Delta x} - e^{-ik(n-1)\Delta x}\right), \qquad \forall\ \alpha = 1..N \tag{23}$$

This result is substituted back into the EoM, together with the expression for $Q(\omega,k)$ (Eq. 13) and the expression found for $A(k,\omega)$ (Eq. 16). The result is

$$-\frac{\omega^2 m}{2\pi\rho_w b}\frac{1}{\Delta x^2}\sum_{n=1}^{N}F_n(\omega)\int_{-\infty}^{\infty}\frac{\lambda\tan(\lambda H)}{k^2}\frac{e^{-ikn\Delta x}-e^{-ik(n-1)\Delta x}}{-\omega^2-g\lambda\tan(\lambda H)}\left(e^{ik\alpha\Delta x}-e^{ik(\alpha-1)\Delta x}\right)dk=\sum_{n=1}^{N}F_n(\omega)+1,\qquad\forall\ \alpha=1..N \tag{24}$$

In this final expression the only unknowns are the F_n's. As there are now also N equations the F_n's can be solved for. Obtaining the solution requires evaluation of the integral due to the inverse Fourier transform over k. This evaluation is done next.

SOLVING THE INVERSE FOURIER INTEGRAL

The integral will be solved using contour integration. First the integral is reformulated

$$\mho(n,\alpha,\omega)=\int_{-\infty}^{\infty}\frac{C(\omega,k)}{DE(k,\omega)}\left(e^{-ikn\Delta x}-e^{-ik(n-1)\Delta x}\right)\left(e^{ik\alpha\Delta x}-e^{ik(\alpha-1)\Delta x}\right)dk \tag{25}$$

$$C(k,\omega)=-\frac{m\omega^2}{2\pi\rho_w b}\frac{1}{\Delta x^2}\lambda\sin(\lambda H),\qquad DE=k^2\cos(\lambda H)\left(-\omega^2-g\lambda\tan(\lambda H)\right) \tag{26}$$

To simplify solving the integral, it is split into four parts

$$\begin{aligned}\mho(n,\alpha,\omega)&=I_{\alpha,n}+I_{\alpha-1,n}+I_{\alpha,n-1}+I_{\alpha-1,n-1}\\&=\int_{-\infty}^{\infty}\frac{C(k,\omega)}{DE(k,\omega)}e^{ik\Delta x(\alpha-n)}\,dk\\&-\int_{-\infty}^{\infty}\frac{C(k,\omega)}{DE(k,\omega)}e^{ik\Delta x((\alpha-1)-n)}\,dk\\&-\int_{-\infty}^{\infty}\frac{C(k,\omega)}{DE(k,\omega)}e^{ik\Delta x(\alpha-(n-1))}\,dk\\&+\int_{-\infty}^{\infty}\frac{C(k,\omega)}{DE(k,\omega)}e^{ik\Delta x((\alpha-1)-(n-1))}\,dk\end{aligned} \tag{27}$$

These four integrals are solved using contour integration. Three cases exist for each integral, resulting in a total of 12 integrals to solve. As the three cases are very similar for all four integrals a general form is solved

$$I_{p_1,p_2}=c_s\int_{-\infty}^{\infty}\frac{C(k,\omega)}{DE(k,\omega)}e^{ik\Delta x(p_1-p_2)}\,dk \tag{28}$$

where c_s is a constant which contains the sign of the original integrals (see Eq. 27). In order to use contour integration, the integrand must evaluate to zero along the complex part of the semi-circle. This means that the integrand, DE^*, must go to zero when k goes to infinity.

$$DE^*=\frac{\lambda\tan(\lambda H)\,e^{ik\Delta x(p_1-p_2)}}{k^2(-\omega^2-g\lambda\tan(\lambda H))} \tag{29}$$

$\lim_{k\to?}$	$\lim_{k\to?}\lambda =$	$\lim_{k\to?}\tan(\lambda H) =$	$\lim_{k\to?} DE^* =$
∞	$\sqrt{\frac{\omega^2}{c^2}-\infty^2} = ik$	$i\tanh(kH) = i$	$\frac{ikie^{ik\Delta x(p_1-p_2)}}{k^2(-\omega^2-giki)} = -\frac{e^{ik\Delta x(p_1-p_2)}}{gk^2} = 0 \rightarrow$ ok
$-\infty$	$\sqrt{\frac{\omega^2}{c^2}-\infty^2} = ik$	$i\tanh(kH) = i$	$\frac{ikie^{-i\infty\Delta x(p_1-p_2)}}{k^2(-\omega^2-giki)} = -\frac{e^{-ik\Delta x(p_1-p_2)}}{gk^2} = 0 \rightarrow$ ok
$i\infty$	$\sqrt{\frac{\omega^2}{c^2}+\infty^2} = k$	$\tan(kH) =$ undefined	$\frac{k\tan(kH)\,e^{-k\Delta x(p_1-p_2)}}{-k^2(-\omega^2-gk\tan(kH))} = \frac{\tan(kH)\,e^{-k\Delta x(p_1-p_2)}}{gk^2\tan(kH)} = \frac{e^{-k\Delta x(p_1-p_2)}}{gk^2} = 0 \rightarrow p_1 > p_2$
$-i\infty$	$\sqrt{\frac{\omega^2}{c^2}+\infty^2} = k$	$\tan(kH) =$ undefined	$\frac{k\tan(kH)\,e^{k\Delta x(p_1-p_2)}}{-k^2(-\omega^2-gk\tan(kH))} = \frac{e^{k\Delta x(p_1-p_2)}}{gk^2} = 0 \rightarrow p_1 < p_2$

Table 1: The integrand evaluated at the various limit cases of k

In order to satisfy the condition at infinity, certain conditions apply to the relation between p_1 and p_2. Two conditions already present themselves in the third and fourth row, namely $p_1 > p_2$ in the upper half plane ($\Im(k) > 0$) and $p_1 < p_2$ in the lower half plane. For the third and last case when $p_1 = p_2$ there are no requirements on which half plane must be used. Despite the absence of a decaying exponent, the integrand still converges to zero for this special case because the denominator is second order in k. With the three cases specified, each is now solved in turn.

Solving case 1: $I_{p_1<p_2}$

I_{p_1,p_2} is solved for the domain where $p_1 < p_2$. As shown before in Table 1, the contour has to be closed over the bottom half plane ($\Im(k) < 0$). Using a clockwise contour integral gives $-2\pi i$ due to the residue theorem. The solution to the integral is

$$I_{p_1<p_2} = -2\pi i c_s \sum_{q=1}^{\infty} \frac{e^{ik_q\Delta x(p_1-p_2)}}{\partial DE/\partial k|_{k=k_q}} C(k_q,\omega), \qquad p_1 < p_2 \tag{30}$$

where k_q are the roots of the dispersion. The integral has been solved but the solution requires the roots of the following dispersion equation

$$DE = k^2\cos(\lambda H)\,(-\omega^2 - g\lambda\tan(\lambda H)) \tag{31}$$

The equation has three sets of roots; one set due to the k^2, one due to the cosine and one due to the terms in the brackets. Each set is analysed

- The k^2 gives two roots which are $k = 0$. The root would cause the entire system (including the fluid) to move as a rigid body which is not realistic for this problem and so this root is not included.
- The cosine has roots when $\lambda H = \pi\left(\frac{1}{2}+\varsigma\right)\ \forall\,\varsigma \in \mathbb{Z}$. However, substituting these roots into the dispersion equation gives

$$k^2(0)\left(-\omega^2 - g\lambda\frac{\sin(\lambda H)}{(0)}\right) = -\omega^2 k^2(0) - k^2 g\lambda\sin(\lambda H) = -k^2 g\lambda\sin(\lambda H) \neq 0$$

Which means that roots of the cosine are not actually roots of the dispersion equation.

- As it turns out, the only roots which are valid are the roots from the last term inside the brackets: $-\omega^2 - g\lambda\tan(\lambda H)$.

These roots can be found numerically. It is important to note that the roots are symmetrical with respect to the origin. This means that if the set of roots from the upper half plane is called $\hat{k}_q$, the ones from the lower half plane would be equal to $-\hat{k}_q$. With this in mind Eq. 30 is updated

$$I_{p_1<p_2} = -2\pi i c_s \sum_{q=1}^{\infty} \frac{e^{-i\hat{k}_q \Delta x(p_1-p_2)}}{\partial DE/\partial k|_{k=-\hat{k}_q}} C\left(-\hat{k}_q, \omega\right), \qquad p_1 < p_2 \tag{32}$$

Solving case 2: $I_{p_1>p_2}$

I_{p_1,p_2} is solved for the domain where $p_1 > p_2$. As shown before, the contour has to be closed over the upper half plane, resulting in a counter-clockwise contour (giving $+2\pi i$)

$$I_{p_1>p_2} = 2\pi i c_s \sum_{q=1}^{\infty} \frac{e^{i\hat{k}_q \Delta x(p_1-p_2)}}{\partial DE/\partial k|_{k=\hat{k}_q}} C\left(\hat{k}_q, \omega\right), \qquad p_1 > p_2 \tag{33}$$

Solving case 3: $I_{p_1=p_2}$

I_{p_1,p_2} is solved for the special case when $p_1 = p_2$. The integral contour is zero independently of whether it is closed over the upper or lower half plane and so the choice of plane is arbitrary. Here the upper plane is chosen due to its flamboyant nature

$$I_{p_1=p_2} = 2\pi i c_s \sum_{q=1}^{\infty} \frac{1}{\partial DE/\partial k|_{k=\hat{k}_q}} C\left(\hat{k}_q, \omega\right), \qquad p_1 = p_2 \tag{34}$$

Solutions to the actual integrals

The same principles which were used to solve the general case also apply to the four actual integrals. Because of thus the answers are directly written down in the table below.

Integral	Half plane	c_s	Quadrant sign	$c_{s,final}$	p_1	p_2	$\hat{k}_{q,signed}$
$I_{\alpha>n}$	Upper	$+1$	$+1$	$+1$	α	n	$+\hat{k}_q$
$I_{\alpha-1>n}$	Upper	-1	$+1$	-1	$\alpha-1$	n	$+\hat{k}_q$
$I_{\alpha>n-1}$	Upper	-1	$+1$	-1	α	$n-1$	$+\hat{k}_q$
$I_{\alpha-1>n-1}$	Upper	$+1$	$+1$	$+1$	$\alpha-1$	$n-1$	$+\hat{k}_q$
$I_{\alpha<n}$	Lower	$+1$	-1	-1	α	n	$-\hat{k}_q$
$I_{\alpha-1<n}$	Lower	-1	-1	$+1$	$\alpha-1$	n	$-\hat{k}_q$
$I_{\alpha<n-1}$	Lower	-1	-1	$+1$	α	$n-1$	$-\hat{k}_q$
$I_{\alpha-1<n-1}$	Lower	$+1$	-1	-1	$\alpha-1$	$n-1$	$-\hat{k}_q$
$I_{\alpha=n}$	Upper	$+1$	$+1$	$+1$	1	1	$+\hat{k}_q$
$I_{\alpha-1=n}$	Upper	-1	$+1$	-1	2	1	$+\hat{k}_q$
$I_{\alpha=n-1}$	Upper	-1	$+1$	-1	1	2	$+\hat{k}_q$
$I_{\alpha-1=n-1}$	Upper	$+1$	$+1$	$+1$	2	2	$+\hat{k}_q$

Table 2: All three cases (>,< and =) for each of the four integrals from Eq. 27.

With this table the solution to any of the twelve integrals can be obtained by making the appropriate substitutions into the following equation

$$I_{p_1,p_2} = 2\pi i c_{s,final} \sum_{q=1}^{\infty} \frac{e^{i\hat{k}_{q,signed}\Delta x(p_1-p_2)}}{\partial DE/\partial k|_{k=\hat{k}_{q,signed}}} C\left(\hat{k}_{q,signed}, \omega\right) \tag{35}$$

Making all the required substitutions and adding everything up gives the following solution to the original inverse Fourier integral (Eq. 25)

$$\begin{aligned} \mho(n,\alpha,\omega) &= \int_{-\infty}^{\infty} \frac{C(k,\omega)}{DE(k,\omega)} \left(e^{-ikn\Delta x} - e^{-ik(n-1)\Delta x}\right)\left(e^{ik\alpha\Delta x} - e^{ik(\alpha-1)\Delta x}\right) dk \\ &= \begin{cases} I_{\alpha-1>n} + I_{\alpha>n} + I_{\alpha>n-1} + I_{\alpha-1>n-1} & \alpha - 1 > n \\ I_{\alpha-1=n} + I_{\alpha>n} + I_{\alpha>n-1} + I_{\alpha-1>n-1} & \alpha = n+1 \\ I_{\alpha-1<n} + I_{\alpha=n} + I_{\alpha>n-1} + I_{\alpha-1=n-1} & \alpha = n \\ I_{\alpha-1<n} + I_{\alpha<n} + I_{\alpha=n-1} + I_{\alpha-1<n-1} & \alpha = n-1 \\ I_{\alpha-1<n} + I_{\alpha<n} + I_{\alpha<n-1} + I_{\alpha-1<n-1} & \alpha < n-1 \end{cases}, \\ &\forall\ \alpha = n = 1..P \end{aligned} \tag{36}$$

This spacious expression can be simplified by observing that the following equality holds for all cases

$$\frac{C\left(-\hat{k}_q, \omega\right)}{\partial DE/\partial k|_{k=-\hat{k}_q}} = -\frac{C\left(\hat{k}_q, \omega\right)}{\partial DE/\partial k|_{k=\hat{k}_q}} = -\Theta \tag{37}$$

This equality is substituted in Eq. 32 and Eq. 33

$$\begin{aligned} I_{p_1<p_2} &= -2\pi i c_s \sum_{q=1}^{\infty} \frac{e^{-i\hat{k}_q\Delta x(p_1-p_2)}}{\partial DE/\partial k|_{k=-\hat{k}_q}} C\left(-\hat{k}_q, \omega\right) = 2\pi i c_s \sum_{q=1}^{\infty} \Theta e^{-i\hat{k}_q\Delta x(p_1-p_2)} \\ &= 2\pi i c_s \sum_{q=1}^{\infty} \Theta e^{i\hat{k}_q\Delta x(p_2-p_1)}, \qquad p_1 < p_2 \end{aligned} \tag{38}$$

$$I_{p_1>p_2} = 2\pi i c_s \sum_{q=1}^{\infty} \frac{e^{i\hat{k}_q\Delta x(p_1-p_2)}}{\partial DE_{\blacksquare}/\partial k|_{k=\hat{k}_q}} C\left(\hat{k}_q, \omega\right) = 2\pi i c_s \sum_{q=1}^{\infty} \Theta e^{i\hat{k}_q\Delta x(p_1-p_2)}, \quad p_1 > p_2 \tag{39}$$

Since p_1 and p_2 both go from $1..P$, they can be interchanged. This means that $I_{p_1<p_2} = I_{p_1>p_2}$ and that $p_1 - p_2$ and $p_2 - p_1$ can be replaced by a new variable Δp which is equal to $|\,p_1 - p_2|$. Using this simplification, the expression for $\mho(n,\alpha,\omega)$ can be greatly simplified. By directly taking into account the signs from Table 2 $\mho(n,\alpha,\omega)$ becomes

$$\begin{aligned} \mho(n,\alpha,\omega) &= \begin{cases} 2I_{\Delta p}(0) - 2I_{\Delta p}(1) & \Delta p = 0 \\ -I_{\Delta p}(\Delta p - 1) + 2I_{\Delta p}(\Delta p) - I_{\Delta p}(\Delta p + 1) & \Delta p = 1..P-1' \end{cases} \\ &\Delta p = |\alpha - \mathrm{n}| \quad \forall \quad n = \alpha = 1..N \end{aligned} \tag{40}$$

With a small tweak the first case be included in the second one. The expression for $\mho(n,\alpha,\omega)$ then reduces to its simplest possible form

$$\begin{aligned} \mho(n,\alpha,\omega) &= -I_{\Delta p}(|\Delta p - 1|) + 2I_{\Delta p}(\Delta p) - I_{\Delta p}(\Delta p + 1), \\ &\Delta p = |\alpha - \mathrm{n}| \quad \forall \quad n = \alpha = 1..N \end{aligned} \tag{41}$$

Solving for $F_n(\omega)$

With the integral solved, the unknown force amplitudes $F_n(\omega)$ can now be solved

$$\sum_{n=1}^{P} F_n(\omega)(\mho(n,\alpha,\omega)-1)=1, \qquad \forall\ \alpha=1..N \tag{42}$$

From this equation a coefficient matrix $\boldsymbol{CFM}$ of size $[N,N]$ can be established with the following entries

$$\boldsymbol{CFM}[n,\alpha](\omega)=\mho(n,\alpha,\omega)-1, \qquad \forall\ \alpha=n=1..N \tag{43}$$

This matrix is symmetric and each diagonal line contains the same value (symmetric Toeplitz matrix) because of the property explained before (Eq. 37). Because of this, only N evaluations of $\mho(n,\alpha,\omega)$ are required to fill the entire matrix. Finally, the following equation is obtained which can be solved for the unknown force amplitudes

$$\boldsymbol{CFM}(\omega)\boldsymbol{F}(\omega)=\mathbf{1} \tag{44}$$

where $\boldsymbol{F}(\omega)$ is a $[N,1]$-vector containing the unknown amplitude of all the interface forces $F_n(\omega)$. Using the following equation, which is based on Eq. 18, the complex frequency response of the body to an impulse load can be obtained

$$\widetilde{W}(\omega)=\frac{(\sum_{n=1}^{N}F_n(\omega))+1}{-m\omega^2} \tag{45}$$

With tis expression the complex frequency domain response of the ice block is known, which concludes the first part of the paper. In the last part of the paper a fast way to compute the time domain response is presented.

NUMERICALIZATION

With the complex-valued FDR known, the time domain response can be obtained using an inverse Fourier integral (Eq. 11) over frequency

$$W(t)=\frac{1}{2\pi}\int_{-\infty}^{\infty}\widetilde{W}(\omega)e^{i\omega t}d\omega \tag{46}$$

This integral can be evaluated in a number of ways. The most straightforward way would be to numerically compute the integral directly. However, that formulation would not be compatible with non-linear forces (e.g. contact forces). Another option would be to calculate the impulse response of the system in the time domain and then use a convolution integral to obtain the response to a non-linear force. This approach is not desirable as it is computationally intense.

The options which will be pursued here is to use numericalization. Before explaining what this means and how it works, the FDR is scaled with respect to the hydrostatic stiffness as this makes the output easier to read. As the system is linear the response can simply be scaled by multiplying it with the scaling factor

$$\widetilde{W}(\omega)=\tilde{F}_{ext}\frac{(\sum_{n=1}^{N}F_n(\omega))+1}{-m\omega^2}, \qquad \tilde{F}_{ext}=1k_{hs} \tag{47}$$

The 1 in the force has a unit of meters. By using numericalization the FDR function of a reference system (in this case that of the floating rigid body given by Eq. 47) is approximated with one of a replacement system whose time domain representation allows for straightforward numerical implementation (Figure 3). The replacement system can then be

used to compute the time-domain response of the reference system. The main advantage is that now an ODE solver can be used instead of having to use a convolution integral.

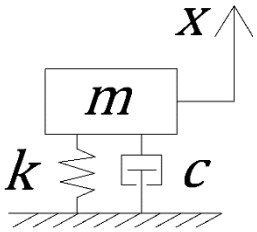

Figure 3: A mass-spring-dashpot system.

Replacement systems

The simplest building block for creating such replacement systems are rigid bodies. As they are inherently discrete, their numerical implementation is trivial, making them perfect for numericalization. To illustrate the idea, a single mass-spring-dashpot (MSD) system is used, see Figure 3. Its EoM is transformed to the frequency domain to obtain its FDR function

$$\hat{m}\ddot{x} + \hat{c}\dot{x} + \hat{k} = \delta(t) \quad \overset{\mathcal{F}}{\rightarrow} \quad -\omega^2\hat{m}\tilde{x} + i\omega\hat{c}\tilde{x} + \hat{k}\tilde{x} = 1 \rightarrow$$
$$\tilde{x} = \frac{1}{\hat{k} - \hat{m}\omega^2 + i\omega\hat{c}} \tag{48}$$

The goal is for the replacement system's FDR (Eq. 47) to be the same as that of the reference system (Eq. 48). As such the following equation should be strived for

$$\tilde{F}_{ext}\frac{(\sum_{n=1}^{N} F_n(\omega)) + 1}{-m\omega^2} = \frac{1}{\hat{k} - \hat{m}\omega^2 + i\omega\hat{c}} \tag{49}$$

This condition can never be satisfied exactly, hence numericalization being an approximation of the FDR. To relax the condition, a frequency range which only contains the first natural frequency of the reference system is considered. As the FDR function of the reference system was normalized, the value for $\hat{k}$ is known and is 1 [N/m]. This leaves two parameters to optimize using an optimization library, namely the mass and the dashpot.

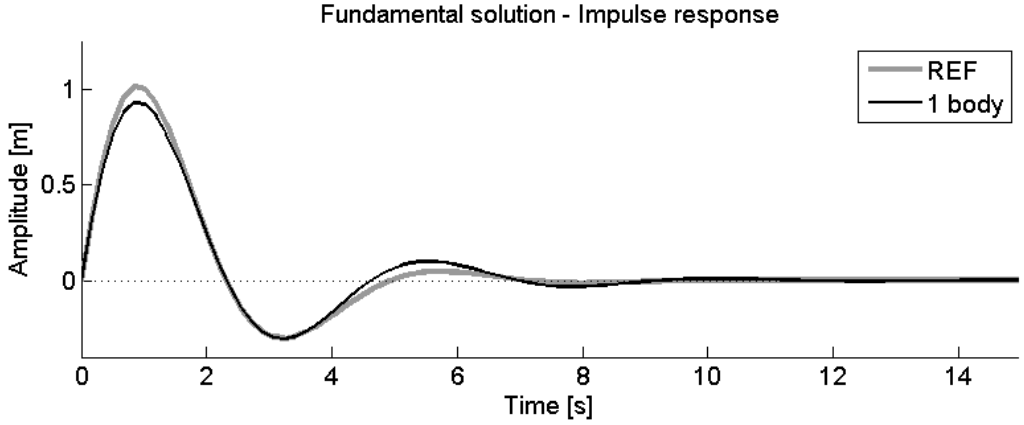

Figure 4: Fitting with a single mass replacement system. The grey line is solution computed using the results from the first part of the paper and the black line the solution computed using the replacement system.

As can be seen, the matching is already quite good even with only a single body. In order to improve the fit, additional frequency dependent parameters need to be introduced to increase the flexibility of the replacement system's FDR function. Although a single body only has

three parameters for matching its complex frequency response to that of the target system, multiple bodies can be connected together to create large discrete systems with greatly increased flexibility. Note that increasing the number of bodies to improve the quality of the fit comes at the cost of increased computation time. Figure 5 shows a two and three body replacement system.

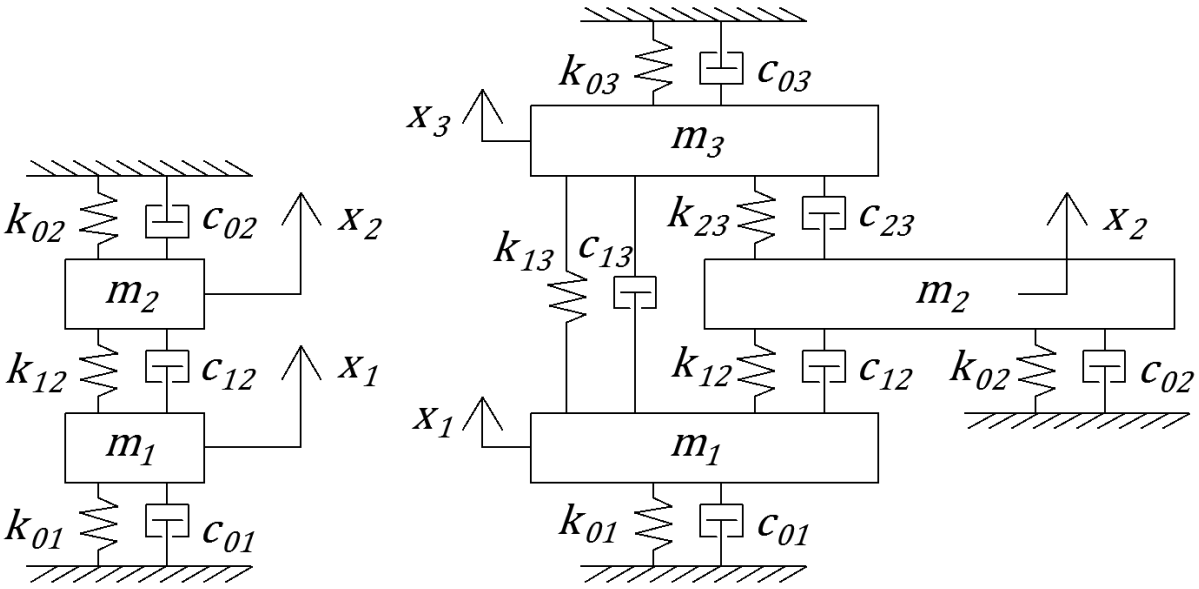

Figure 5: Adding an additional body increases the flexibility of the replacement system from 3 parameters to 7. A third body adds an additional 8.

With these extra bodies there are additional degrees of freedom (DOF) in the replacement systems, namely x_2 and x_3. Despite these DOF having a displacements and a velocity, they have no physical meaning. Their only purpose is to increase the flexibility of the FR function of the main DOF (x_1) by increasing the number of parameters in its FR functions which can be used for fitting. Only the state of x_1 has a physical meaning as only the FR of this body is matched to that of the reference system.

RESULTS

Figure 6 shows the fit for replacement system of one, two and three bodies. The three body system has an overall error of about 1 mm (or 0.1%) compared to the impulse response of the reference system shown in Figure 4.

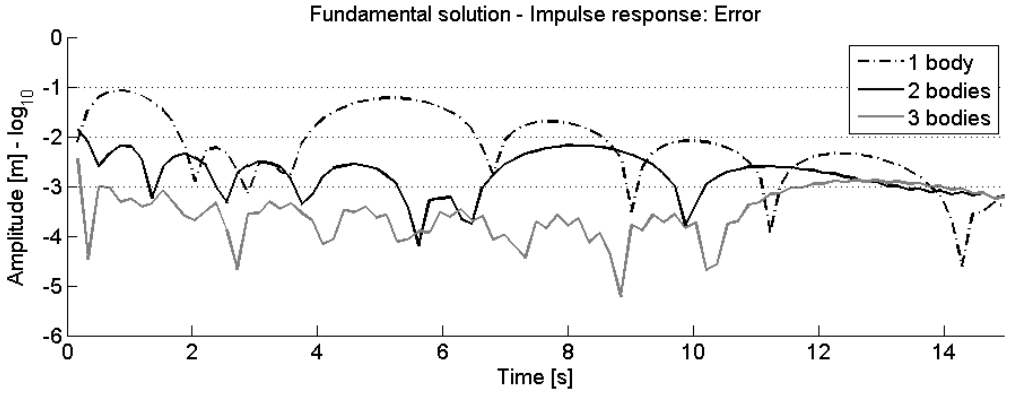

Figure 6: Fit quality using a replacement systems of 1,2 and 3 bodies. The error is absolute difference between the exact solution derived in the first part of the paper and the various replacement systems introduced as depicted in Figure 5 and Figure 6.

From these results it can be seen that the heave motions of the ice block can be replaced by a system with three bodies and the error will be minimal. The same can be for the pitch motion using the same procedure. In total this will result in a system with about 7 bodies. This replacement system can then be used to calculate the time-domain response of the ice block when subjected to nonlinear loading, greatly improving the speed compared to using convolution integrals.

CONCLUSION AND RECOMMENDATIONS

The methodology showcased in this papers results in a numerically efficient way to compute the response of a floating ice block whilst incorporating the effects of hydrodynamics. An replacement system with only three degrees of freedom is already sufficient to accurately capture the behaviour of the floating body. Solving three bodies with an ODE solver to compute the time domain response is much faster than using a convolution integral, providing a significant boost in calculation time.

This paper introduced the methodology for the case of a rigid body. Future work will focus on extending the methodology to get a time domain representation of a flexible beam of finite length.

REFERENCES

Environment, S., Lu, W., Løset, S., & Lubbad, R. (2012). 21 st IAHR International Symposium on Ice Ventilation and Backfill Effect during Ice-sloping Structure Interactions, 826–841.

Gagnon, R. E., & Wang, J. (2012). Numerical simulations of a tanker collision with a bergy bit incorporating hydrodynamics, a validated ice model and damage to the vessel. *Cold Regions Science and Technology*, *81*, 26–35. doi:10.1016/j.coldregions.2012.04.006

Isaacson, M., & McTaggart, K. A. (1990). Modelling of iceberg drift motions near a large offshore structure. *Cold Regions Science and Technology*. doi:10.1016/0165-232X(90)90017-Q

Keijdener, C., & Metrikine, A. V. (2014). The effect of ice velocity on the breaking length of level ice failing in downward bending. *Proceedings of 22nd IAHR International Symposium on Ice*.

Kim, E., Storheim, M., von Bock und Polach, R., & Amdahl, J. (2012). Design and Modelling of Accidental Ship Collisions With Ice Masses at Laboratory-Scale. *Volume 6: Materials Technology; Polar and Arctic Sciences and Technology; Petroleum Technology Symposium*, 495. doi:10.1115/OMAE2012-83544

Squire, V. A. (2007). Of ocean waves and sea-ice revisited. *Cold Regions Science and Technology*. doi:10.1016/j.coldregions.2007.04.007

Tsarau, A., Lubbad, R., & Løset, S. (2014). A numerical model for simulation of the hydrodynamic interactions between a marine floater and fragmented sea ice. *Cold Regions Science and Technology*, *103*, 1–14. doi:10.1016/j.coldregions.2014.03.005